LUND UNIVERSITY

Thermodynamic description of the Au-In-Ga ternary system based on the CALPHAD method

Ghasemi, Masoomeh

2014

Licentiate Thesis

Thermodynamic description of the Au-In-Ga ternary system based on the CALPHAD method

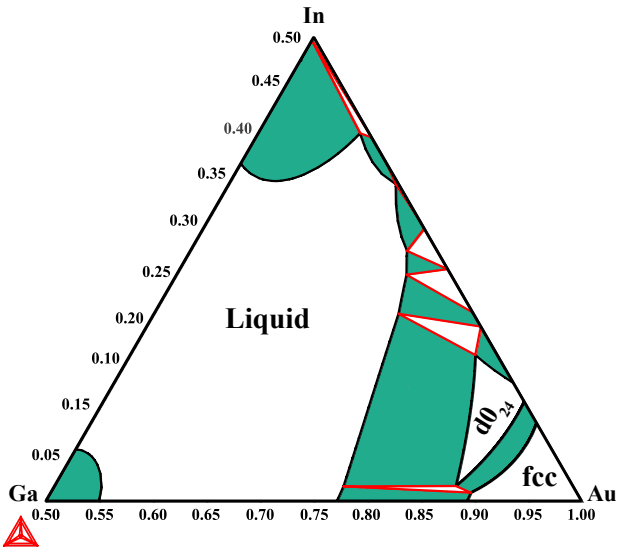

Masoomeh Ghasemi

Division of Solid State Physics
Department of Physics
Lund University, Sweden

2014

Licentiate Thesis

Thermodynamic description of the Au-In-Ga ternary system based on the CALPHAD method

Author:
Masoomeh Ghasemi

Supervisor:
Prof. Jonas Johansson

Division of Solid State Physics
Department of Physics
Lund University

2014

Division of Solid State Physics
Department of Physics
Lund University
Box 118
S-22100 Lund
Sweden

ISBN 978-91-7623-028-2 (print)
ISBN 978-91-7623-029-9 (pdf)

Printed in Sweden by Media-Tryck, Lund University
Lund, 2014

Abstract

There has recently been a considerable attention to the possible role of semiconductor nanowires for future device applications. To make this development feasible, precise control over the growth mechanism is required. In the Vapor-Liquid-Solid growth, the most common growth mechanism, gas phase precursors decompose in presence of catalytic particles and after supersaturating the particles, solid nanowires start to nucleate and grow from the seed particle. The knowledge on the equilibrium state of the seed particle is useful to understand the growth mechanism.

In this work, we investigated the thermodynamic description of the Au-In-Ga ternary system by calculating its phase diagram. Using this phase diagram, the state of the gold particles in Au-seeded nanowires containing In and Ga can be explained. The phase diagram was investigated experimentally and computationally. The most common technique for calculating phase diagrams, the CALPHAD technique, was used for the calculations. The measurements on the system were performed using relevant thermal, crystallographic, structural and compositional analysis techniques. The most important results of the measurements were the identification of a new ternary phase, the ternary solubilities and the phase transition temperatures. These enabled us to optimize the calculated phase diagram and hence the thermodynamic description of the system.

Contents

List of Papers

This thesis is based on the following articles:

I. Bonding in intermetallics may be deceptive- The case of the new type structure Au_2InGa_2
Masoomeh Ghasemi, Sven Lidin, Jonas Johansson and Fei Wang. Intermetallics, 46, 40-44, 2014.

II. The phase equilibria in the Au-In-Ga ternary system
Masoomeh Ghasemi, Sven Lidin and Jonas Johansson. Journal of Alloys and Compounds, 588, 474-480, 2014.

III. The thermodynamic assessment of the Au-In-Ga system
Masoomeh Ghasemi, Bo Sundman, Suzana G. Fries and Jonas Johansson. Journal of Alloys and Compounds, 600, 178-185, 2014.

The following article is not included in the thesis, however it is related to the application of the Au-In-Ga phase diagram in the growth of nanowires:

IV. Morphology and Composition Controlled $Ga_xIn_{1-x}Sb$ Nanowires: Understanding Ternary Antimonide Growth
S. Gorji Ghalamestani, M. Ek , M. Ghasemi, P. Caroff, J. Johansson, K.A. Dick. Nanoscale, 6(2), 1086-92, 2014.

List of Abbreviations and Notations

μ_j	chemical potential of component j
CALPHAD	CALculation of PHAse Diagrams
CEF	Compound Energy Formalism
DSC	Differential Scanning Calorimetry
DTA	Differential Thermal Analysis
EDS	Energy Dispersive X-ray Spectroscopy
SEM	Scanning Electron Microscopy
SGTE	Scientific Group Thermodata Europe
VLS	Vapor-Liquid-Solid
XRD	X-Ray Diffraction
C_p	heat capacity
G	Gibbs energy
H	enthalpy
L	interaction parameter
n_i	composition of component i
P	pressure
S	entropy
T	temperature

Acknowledgements

I feel lucky to have the opportunity of working with very talented and supportive people during the two first years of my PhD studies. It would not be possible to write this licentiate without their support.

First of all, I want to give my special thanks to my main supervisor, Dr. Jonas Johansson. Thanks for giving me the chance of doing this PhD program and for all your support.

I am extremely grateful to Prof. Sven Lidin for teaching and helping me to use XRD and DTA setup. I never forget how excited we got about detecting the new ternary phase. Thanks for all the discussions we had together. Hereby, I also acknowledge Dr. Fei Wang, for the calculations on the electronic structure of the ternary compound.

Sören Jeppesen, thanks for the technical support and especially for making a nice setup for sealing the quartz tubes. I always enjoy our daily chats.

Prof. Bo Sundman and Dr. Suzana Fries are gratefully acknowledged for helping me with the assessment. Thanks for your invaluable comments, corrections and recommendations. I look forward to have more collaborations with you.

I also acknowledge the support I received from my assistant supervisor, Dr. Kimberly Dick.

I would also like to thank Prof. Reine Wallenberg and Gunnel Karlsson at nCHREM for the opportunity to use their EDS and SEM setup. Thank you Gunnel for teaching me to use the setup.

Dr. Volodymyr Bushlya is acknowledged for helping me with polishing my samples at their lab at the M-building.

Thanks to my nice friends and colleagues at Solid State Physics divi-

sion, Chemical center and Mechanical engineering department. Thank you Carola Muller, Hossein Sina, Ritayan Chatterjee, Sepideh Gorji, Daniel Jacobsson and Håkan Lapovski for always being available to help me out.

I am also grateful to all people at Solid State Physics division for making a welcoming environment.

Special thanks goes to my parents, my brothers and my second family for their constant support and encouragement over these years.

Last but the most of all, thanks to my husband, Abbas. Thanks for encouraging me to follow my studies and for bearing with me to live far from you during this period.

Masoomeh Ghasemi
Lund University
9 April 2014

Chapter 1

Introduction

One dimensional nanoscale structures, so called nanowires, are promising building blocks of future devices. Semiconductor nanowires are of special interest for fabrication of scaled electronic and photonic devices such transistors, LEDs and lasers [1,2]. The common growth mechanism of nanowires is through the VLS (Vapor-Liquid-Solid) growth [3]. In VLS, seed particles (often Au nanoparticles) are deposited on a crystalline substrate. At elevated temperatures, the nanowire precursors in gas phase (e.g. metalorganics in case of metalorganic vapor phase epitaxy) are introduced to the growth chamber and decompose at the seed particle surface which is in liquid state. After supersaturation of the seed particles, the nanowirses begin to crystallize at the interface between the seed particle and the substrate. To grow defect-free nanowires, a comprehensive understanding of the growth mechanism and the control over the growth parameters are essential.

The VLS mechanism is a kinetically-driven process meaning that a deviation from the equilibrium state of the system is needed to drive the solidification. But a non-equilibrated system tends to recover the equilibrium state when the driving force is removed. Hence, the knowledge of the thermodynamics of a system which here is a description of the equilibrium state of the system is useful for understanding the growth mechanism. In addition, for a small deviation from equilibrium, local equilibria can be assumed at the liquid-solid interface between the seed particle and the growing nanowire [4].

The thermodynamics of a system, either single-component or multicomponent, can be displayed in the phase diagram of that system. A phase diagram is a graphical representation of the relative stability of the co-

existing phases under equilibrium condition as a function of temperature, pressure or composition.

In this work, we have assessed the phase diagram of the Au-In-Ga ternary system based on the CALPHAD technique [5]. The system was also measured using relevant techniques for collecting phase diagram data. The phase diagram of this materials system is useful in understanding the equilibrium state of the Au-particle when growing Au-seeded III-V heterostructure nanowires containing Ga and In, e.g. Au-seeded axial heterostructure GaAs/InAs nanowires [6, 7] or ternary $Ga_xIn_{1-x}As$ nanowires [8]. Note that the Au-In-Ga-As materials system includes arsenic from group V, but due to negligible solubility of As in gold, its role has not been taken into account at this step.

It is noteworthy to mention that for a nanoscale system, however, the confined size of the system gives rise to pronounced surface effects causing melting point depression and shifting the phase boundaries. This has been shown in several theoretical [9–13] and experimental [14–16] studies of the phase diagram of nanomaterial systems. It implies that to have an optimized description of thermodynamics of a nanowire system, the size effect should also be considered. Nevertheless, the current assessment is still relevant for nanowires thicker than 100 nm in diameter.

We first extrapolated the Au-In-Ga phase diagram from the constituting binaries, Au-Ga [17], Au-In [18] and In-Ga [19]. Next, an isothermal section of the phase diagram at 280 °C was calculated and based on that a number of alloy compositions were chosen for measurements. The samples were characterized by complementary techniques including Differential Thermal Analysis (DTA), powder and single-crystal X-Ray Diffraction (XRD), Scanning Electron Microscopy (SEM) and Energy Dispersive X-ray Spectroscopy (EDS). The measurements revealed the presence of a previously unknown ternary phase, Au_2InGa_2, and the solubility levels of the binary phases. The description of the system were finally optimized using the experimental results.

The structure of the thesis is as following. In **chapter 2**, principles of the CALPHAD technique which was used for calculating the phase diagram are described. In **chapter 3**, the experimental techniques implemented for

measuring the Au-In-Ga ternary system are discussed. In **chapter 4**, the results of the measurements and the assessment of this system are briefly explained. Finally, in **chapter 5**, the implications and the future aspects of the current research are discussed.

Chapter 2

CALPHAD

The word CALPHAD stands for CALculation of PHAse Diagrams and as is obvious from the name, CALPHAD is a technique for calculating phase diagrams [5, 20]. The calculation of the phase diagrams was initiated by Van Laar [21, 22] in the early years of the 20th century. He implemented the ideal and regular solution models [23] of the Gibbs energy to calculate the phase diagram of binary systems. Later, in 1970, Kaufman and Bernstein [20] developed the concept of *lattice stability* (will be discussed in Section 2.2.1) which is a core concept of the CALPHAD technique. This concept and the development of phase diagram assessments based on experimental data led to calculation of phase diagrams of binary and ternary systems using computer simulations for the first time. In this chapter using the considerations and recommendations of the book *Computational thermodynamics: the CALPHAD method* by Lukas et al. [5]: first, the principles of the CALPHAD technique will be discussed. Next, the models of Gibbs energy of phases will be introduced. Finally, the optimization procedure will be briefly discussed.

2.1 CALPHAD Methodology

Within the CALPHAD method, the thermodynamic description of a multicomponent system is calculated incorporating the phase diagram data, thermochemical data and the crystallographic and physical properties of the phases. Due to the fact that most experiments are performed at constant temperature (T) and pressure (P), the Gibbs energy (G) of phases which is only a function of composition at constant T and P, is modelled using the available experimental and theoretical data. Several model pa-

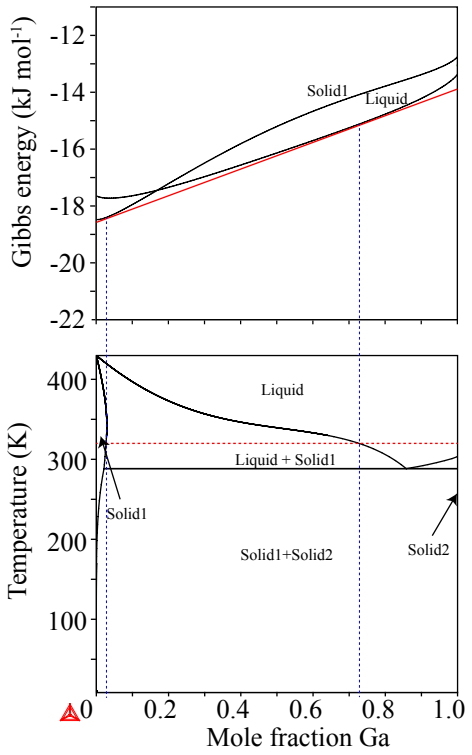

Figure 2.1: The Gibbs energy curves of the phases in the Ga-In system are plotted at T=320 K against the Ga composition. The stability range of single- and two-phase regions are determined by drawing the common tangent (shown with solid red line) of the coexisting curves. At T=320 K, at low concentration of Ga below 2.5 at.%, the single phase *solid1* is stable. Then both *liquid* and *solid1* phases coexist for Ga compositions between 2.5 and 73 at.% Ga. At compositions above 73 at.% Ga, the only stable phase is the *liquid* phase. At this temperature, the phase *solid2* is not stable and its G-curve is located above the other two curves (not shown here). By calculating the G-curves at different temperatures, the temperature-composition ($T - X$) diagram can be mapped as shown in the bottom plot.

rameters are introduced for the Gibbs energy descriptions and they are adjusted to the experimental data. A phase diagram is then constructed by calculating the Gibbs energies of different phases at constant T and P and finding the stable phase as a function of composition (Fig. 2.1).

After calculating the Gibbs energy, G, all other thermodynamic functions can be derived from the Gibbs energy function including:

Entropy:

$$-S = \left(\frac{\partial G}{\partial T}\right)_{P,N_i}$$

Enthalpy:

$$H = G - T\left(\frac{\partial G}{\partial T}\right)_{P}$$

Chemical potential:

$$\mu_j = \left(\frac{\partial G}{\partial N_j}\right)_{T,P,N_{i\neq j}}$$

Heat capacity:

$$C_p = -T\left(\frac{\partial^2 G}{\partial T^2}\right)_{P}$$

where N_i is the composition of component i.

The schematic in Figure 2.2 summarizes the CALPHAD methodology for developing thermodynamic databases. As the first step of the database assessment, a through literature search is performed to find: the experimentally measured thermodynamic quantities such as enthalpies and heat capacity data, the phase diagram data such as the liquidus temperatures and the phase transition reactions, crystallographic information of solid phases [24] and first-principles calculations of total energies [25]. One might also find previous assessments of the same system. In such a case, the possibilities of improving the existing description should be carefully investigated. It is also recommended to find the assessed phase diagram of similar systems. This makes the justification of the Gibbs energy models of phases in the current system easier.

After careful analysis of the data, the model of the Gibbs energy for each phase is suggested using the crystal structure of the phase. The details of phase models will be discussed in Section 2.2. Based on the selected model, a number of model parameters are defined that are to be fitted to the experimental data and calculated total energies. The adjustment of the model parameters is called *optimization* or *assessment*.

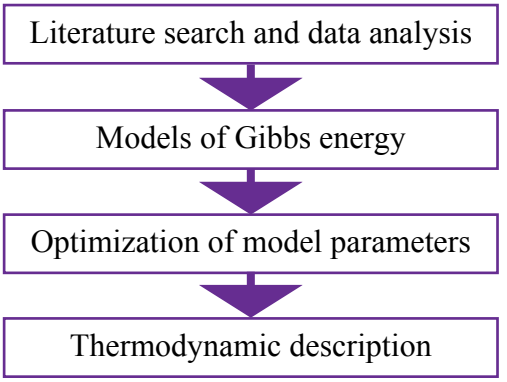

Figure 2.2: CALPHAD methodology.

Finally, an optimized description of the system is obtained that can reproduce the experimental data and can be used to calculate thermodynamic quantities and the phase diagram of the system. The power of the CALPHAD is in that the phase diagram of a higher-order system can be extrapolated from the optimized descriptions (also called databases) of the constituting sub-systems with a minimal need of measuring the higher-order system.

2.2 Models of Gibbs Energy

In a heterogeneous system, chemically or physically distinct regions are called *phases*. A system can consist of a single specie (single-component) or more than one species (multi-component). Note that a component can

be an element or a compound. Phase *constituents* are species that form the phase. In this section the models of Gibbs energy of phases are explained. We first describe the general form of the Gibbs energy function. Next, the models adapted for phases will be discussed. These phases are stoichiometric phases which have fixed composition, solution phases with all species mixing on one sublattice and phases with more than one sublattice. Moreover, the *Compound Energy Formalism (CEF)* [26] which is used for modeling phases with more than one sublattice and with compositional variation on sublattices will be described. Also, the concept of *lattice stability* [27] will be explained.

A model is adapted for a phase based on the information on the crystal structure of the phase, site occupancies and the Wyckoff positions of the constituents. Model parameters like excess energy terms are then introduced for each phase. The parameters consist of several coefficients and can be a function of temperature, pressure and composition.

The general form of the Gibbs energy model is expressed as [5]:

$$G_m^\theta = {}^{\mathrm{srf}}G_m^\theta + {}^{\mathrm{phy}}G_m^\theta - T.{}^{\mathrm{cnf}}S_m^\theta + {}^{\mathrm{E}}G_m^\theta \tag{2.1}$$

where ${}^{\mathrm{srf}}\mathrm{G}_m^\theta$ refers to the Gibbs energy of a mechanical mixture of all the species that form the phase. The contribution of a physical model like for a magnetic phase to the Gibbs energy is described by the ${}^{\mathrm{phy}}G_m^\theta$ term. The third term refers to the configurational entropy and is the number of possible arrangements of the phase constituents. The last term, ${}^{E}G_m^\theta$, is the excess energy term taking into account the interaction between the phase constituents.

2.2.1 Pure elements and stoichiometric phases

The temperature dependency of the molar Gibbs energy, G_m, of a phase θ with a fixed composition (an elemental or a stoichiometric phase) is described by:

$$G_m^\theta - \sum_i b_i H_i^{\mathrm{SER}} = a_0 + a_1 T + a_2 T \ln(T) + a_3 T^2 + a_4 T^{-1} + a_5 T^3 + ... \tag{2.2}$$

where H_i^{SER} is the enthalpy of element i in its reference state, i.e. its stable form at 298.15 K and 1 bar and b_i is the stoichiometric coefficient. For constituting elements (also called *end members*), the a_i coefficients are taken from the SGTE (Scientific Group Thermodata Europe) thermodynamic database [28].

Lattice stability: the metastable structure of the end members can also be described by a similar power series in temperature. The difference between the the Gibbs energy of the phase in its stable structure and the metastable state of the phase is called *lattice stability* [27]. The a_i coefficients for the lattice stability can also be taken from the SGTE database. The reason to take the metastable states into account is that the end member may have considerable solubility in other phases.

Kopp-Neumann rule: the Gibbs energy of the stoichiometric phases has the same expression as a pure element (Eq. 2.1) if the heat capacity of the compound as a function of temperature is measured. Otherwise, the Kopp-Neumann rule is applied. The heat capacity of a compound is estimated from the heat capacities of the pure elements. Only the two first coefficients in Eq. 2.1 will then be optimized using the experimental data:

$$G_m^{\theta} - \sum b_i G_i^{\mathrm{SER}} = a_0 + a_1 T \tag{2.3}$$

2.2.2 Substitutional solution phases

In solutions phases with composition variation, the deviation from the ideal solution is expressed by the excess energy terms:

$$^{E}G_m = {}^{\mathrm{E,bin}}G_m + {}^{E,\mathrm{ter}}G_m + {}^{E,\mathrm{hig}}G_m \tag{2.4}$$

where ${}^{E,\mathrm{bin}}G_m$, ${}^{E,\mathrm{ter}}G_m$ and ${}^{E,\mathrm{hig}}G_m$ are the binary, ternary and higher-order excess energy terms, respectively. ${}^{E}G_m$ is the energy difference between the Gibbs energy of a phase and all other contributing terms rather than the excess energy (the surface of references, the physical contribution and the configurational entropy) in Eq. 2.1.

The binary and ternary excess energies are expressed as:

$$^{E,\text{bin}}G_m = \sum_{i=1}^{n-1} \sum_{j=i+1}^{n} x_i y_j L_{ij} \tag{2.5}$$

$$^{E,\text{ter}}G_m = \sum_{i=1}^{n-2} \sum_{j=i+1}^{n-1} \sum_{k=j+1}^{n} x_i y_j x_k L_{ijk} \tag{2.6}$$

where x_i, x_j and x_k are the mole fractions of constituent i, j and k, respectively. L_{ij} and L_{ijk} are called the binary and ternary interaction parameters, respectively, and are related to the bond energy between similar and dissimilar atoms in a solution. The interaction parameter usually consists of two coefficients[1], i.e. there is a linear temperature-dependency:

$$L = a + bT \tag{2.7}$$

where a and b are related to the excess enthalpy and the excess entropy, respectively. The solution is called a *regular solution*, if the interaction parameter is temperature-independent ($b = 0$). The binary and ternary interaction parameters in Eqs. 2.5 and 2.6 can be expanded using the Redlich-Kister polynomials [29] as following:

$$L_{ij} = \sum_{v=0}^{k} (x_i - x_j)^v \ {}^v L_{ij} \tag{2.8}$$

$$L_{ijk} = v_i \ {}^i L_{ijk} + v_j \ {}^j L_{ijk} + v_k \ {}^k L_{ijk} \tag{2.9}$$

where:

$$v_i = x_i + \frac{1 - x_i - x_j - x_k}{3}$$

$$v_j = x_j + \frac{1 - x_i - x_j - x_k}{3}$$

$$v_k = x_k + \frac{1 - x_i - x_j - x_k}{3}$$

[1] Only if there is experimental data on excess heat capacity, higher-order terms should be used [5].

The sum of v_i, v_j and v_k is equal to unity and guarantees the symmetrical behaviour of the ternary interaction parameter when extrapolating to higher-order systems. Obviously, in the case of a three-component system, v_i, v_j and v_k are the mole fractions of the components. This ternary extrapolation method is called the Redlich-Kister-Muggianu method [30]. There are several other extrapolation methods which will not be discussed here but the interested reader is referred to Refs. [31, 32].

2.2.3 Sublattice model

The sublattice model is used for phases with more than one sublattice. If there is only one constituent on each sublattice, the phase is stoichiometric. For instance, the A_2B compound is modelled with two sublattices and the notation is $(A)_{2/3}(B)_{1/3}$. The first sublattice is occupied by component A and the second one is occupied by component B. Stoichiometric phases are described either by Eq. 2.2 if there is heat capacity measurements or otherwise by the Kopp-Neumann rule as in Eq. 2.3.

Phases with more than one subblattice and with compositional variations on the sublattices should be treated differently. A formalism called *Compound Energy Formalism (CEF)* has been developed by Hillert [26] to model the solution phases with more than one sublattice.

In CEF, instead of mole fraction x_i, the site fractions are used:

$$y_i^{(s)} = \frac{N_i^{(s)}}{N^{(s)}} \tag{2.10}$$

where $N_i^{(s)}$ is the number of sites occupied by constituent i on sublattice s and $N^{(s)}$ is the total number of sites on sublattice s. The mole fraction can be found form the site fraction by:

$$x_i = \frac{\sum_j b_{ij} y_j}{\sum_k \sum_j b_{jk} y_j} \tag{2.11}$$

where b_{ij} coefficient is the stoichiometric factor of component i in constituent j.

An example of CEF is to model the *reciprocal solutions* [5]. A reciprocal solution consists of two sublattices with two constituents on each sublattice: $(\mathrm{A,B})_a(\mathrm{C,D})_b$ where a and b are the ratio of sites on sublattice 1 and 2, respectively. The constituents A, B, C and D can be atoms, ions or even defects like anti-sites and vacancies. For such a solution, the surface of references (${}^{\mathrm{srf}}G_m^\theta$) consists of four compounds: AC, AD, BC and BD. Also, the configurational entropy term differs from that of a substitutional solution where all constituents mix on only one sublattice (${}^{\mathrm{cnf}}S_m^\theta$). In this case, the total configurational entropy is the weighted average of ideal entropies on each sublattice with respect to the stoichiometric coefficients. The Gibbs energy of a reciprocal solution will then be:

$$\begin{aligned} G_m^\theta &= {}^{\mathrm{srf}}G_m^\theta - T.{}^{\mathrm{cnf}}S_m^\theta + {}^{E}G_m^\theta \\ &= y_A^1\ y_C^2\ {}^0G_{A:C} + y_A^1\ y_D^2\ {}^0G_{A:D} + y_B^1\ y_C^2\ {}^0G_{B:C} + y_B^1\ y_D^2\ {}^0G_{B:D} \\ &+ aRT\ [y_A^1\ \ln y_A^1 + y_B^1\ \ln y_B^1] + bRT\ [y_C^2\ \ln y_C^2 + y_D^2\ \ln y_D^2] \\ &+ y_A^1\ y_B^1\ y_C^2\ L_{A,B:C} + y_A^1\ y_B^1\ y_D^2\ L_{A,B:D} + y_A^1\ y_C^2\ y_D^2\ L_{A:C,D} \\ &+ y_B^1\ y_C^2\ y_D^2\ L_{B:C,D} + y_A^1\ y_B^1\ y_C^2\ y_D^2\ L_{A,B:C,D} \end{aligned} \tag{2.12}$$

where the last five terms represent the excess energy terms and y^1 and y^2 are site fractions on the sublattice 1 and 2, respectively. The interaction parameters are represented by Redlich-Kister power series the same as Eqs. 2.8 and 2.9. Obviously, the surface of references (${}^0G$ terms in Eq. 2.12) contribute more to the Gibbs energy function than the excess energy terms because they are multiplied by a smaller number of fractions (y^i).

It should be noted that CEF can be applied to more complicated phases (e.g. phases with more than two sublattices with three or more species mixing on each sublattice) and phases exhibiting phenomena like order/disorder transition. But in this chapter, only the Gibbs energy models relevant to the assessment of the Au-In-Ga system have been discussed.

2.3 Optimization Procedure

To give an overview of the assessment, in this section the procedure is briefly described. For a detailed description, the reader is referred to Refs. [5, 33]. The assessment methodology is explained based on the PARROT optimization module [34] of the Thermo-Calc software [35] which was used in this work.

After assigning the Gibbs energy models to all phases and selecting the adjustable parameters, a setup file including all these is prepared. The setup file should include Gibbs energy functions of pure elements and all phases which are described by the adapted models. Experimental info are assembled in another file, the so called POP file. A work file (the PAR file) is created using the setup file, and the experimental file is compiled within the work file. The PARROT optimizer works based on the least squares method and attempts to fit the model parameters to the experimental data. Therefore, an assessor should select the best set of experimental data and discard conflicting ones during the assessment. They may be later used for comparison. However, it depends on the justification of the assessor to decide which piece of data is more trustworthy.

In the beginning of the assessment, a number of key experimental data with a minimum possible number of model parameters are used. After obtaining the main features of the phase diagram, more experimental data is included and more parameters can be adjusted. The judgement of the assessor plays a significant role during the optimization, because the assessor should select the best set of experimental data and decide on the crucial parameters to be optimized.

It is also worth mentioning that the thermochemical data (e.g., heat capacity or heat content measurements) are very helpful to obtain a thermodynamic description that matches the reality and not only gives a well-fitted phase diagram. Because, even without the thermochemical data a good description of the system can be achieved by adjusting the parameters, but reproduced thermodynamic quantities (e.g. the enthalpy of formation of a stoichiometric phase) from that database may deviate from the real values of these quantities.

Chapter 3

Experimental Techniques

In this chapter, the relevant experimental techniques for collecting phase diagram data are discussed following the recommendations of Ref. [36]. In Section 3.1, the sample preparation procedure and considerations are explained. In the next sections the principles of thermal analysis (Section 3.2), crystallographic analysis (Section 3.3) and microstractural and compositional analysis (Section 3.4) along with the implemented techniques for determination of Au-In-Ga phase diagram are discussed.

3.1 Sample preparation

To investigate the the whole composition range or a region of interest of a phase diagram, first several alloy compositions are selected. The alloys are prepared by mixing weighed pieces of the starting materials. Next, the samples are melted. There are different melting techniques including high temperature melting, arc melting and induction melting. It is also common to use a mixture of powders of the raw materials. But since in the current research we used high temperature melting technique, the considerations regarding this technique will be outlined in this section.

To make sure that all components are melted, the melting temperature is chosen to be the highest melting temperature of the raw materials. Melting at high temperatures needs special cautions to prevent contamination and oxidation of the alloys. To fulfil this, the sample containers (often quartz tubes) are evacuated. The evacuated container can then directly be sealed or be filled by an inert gas like Ar before being sealed. The weight loss is another important issue to be aware of, especially for alloys with volatile constituents. Therefore, the weight of the samples after melting

should be checked.

After melting, the alloys are often homogenized at a high temperature (about 50 °C below the solidus) for a sufficiently long time. The homogenization period depends on the annealing temperature. The lower the temperature, the longer the annealing time[1]. The heat treatment step is to make sure that sample has reached equilibrium.

Thereafter, the sample is either quickly quenched or slowly cooled down to room temperature. Both cooling methods have pros and cons. With quenching, the high temperature phases can be frozen, thus making the investigation of the equilibrium state of the system possible. While the high cooling rate in quenching induces thermal stress in the sample, slow cooling down prevents high levels of stress. This makes the latter method suitable for lattice parameter measurements [36].

3.2 Thermal analysis

Phase transitions can be detected by thermal analysis methods because they are accompanied by release or adsorption of heat. The two most-often-used techniques are Differential Thermal Analysis (DTA) and Differential Scanning Calorimetry (DSC) [36]. In DTA, the temperature difference between a test sample and a reference sample is recorded during a programmed cooling or heating period under the same conditions. The reference sample that can be an empty crucible or a pure element remains in a single phase in the measured temperature range. For the test sample, at the phase transition temperature, an exothermic or endothermic peak (corresponding to release or absorption of the heat, respectively) appears in the temperature curve.

[1]There is no precise recommendations for the annealing duration because it depends on the diffusion properties of the constituents and also on the type of the reaction [36]. Another limiting factor is time limitations of a specific research. In the current research the samples were annealed at 280°C. The duration for a number of samples was 5 days and for the rest it was 26 days. Refer to Table 1 in Paper II [37]. The samples exhibiting the peritectic formation of the ternary phase Au_2InGa_2 did not reach equilibrium even after 26 days of annealing (Fig. 2 of the same paper), though most of the samples annealed for 5 days reached the equilibrium (Fig. 3 of the same paper).

In DSC, the energy required for the transition is measured as a function of temperature or time. Therefore, it is also possible to perform calorimetric measurements such as enthalpy and heat content. We used the DTA technique for thermal analysis.

The heating/cooling rate, the sample size and furnace environment are factors affecting the DTA results [36]. The typical heating/cooling rate is 10 °C/min but depending on the sample properties lower or higher rates may be used. The desired sample mass for the DTA measurements is a few hundred milligrams. Using an inert carrier gas in the furnace prevents oxidation and contamination. For detailed explanation on the effect of the mentioned factors on the recorded DTA curves, the reader is referred to Ref. [36, 38].

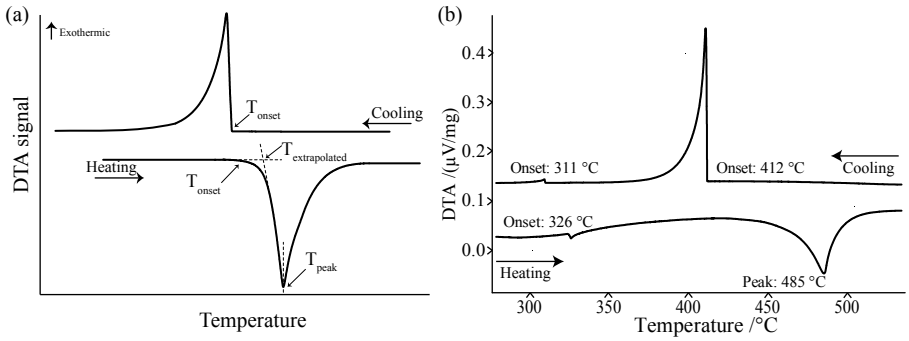

Figure 3.1: (a) Heating and cooling DTA signal of a pure element. Reproduced and modified with permission from [36], © Elsevier 2007. (b) DTA signals of a multiphase sample with the composition of 50.0% Au, 45.1% In, 4.9% Ga. The heating/cooling rate is 10 °C/min.

A DTA signal of a pure element on heating and cooling is shown in Fig. 3.1-a. Three temperatures: T_{onset}, T_{peak} and $T_{\text{extrapolated}}$ are distinguished on the heating curve. On heating, the beginning of the deviation from the baseline of the curve which is equivalent to the onset of the melting is the onset temperature (T_{onset}). Due to difficulty in determining the T_{onset},

the onset of thermal event (melting in this case) is usually extrapolated. The corresponding temperature on the DTA signal is the $T_{\text{extrapolated}}$. T_{peak} shows the maximum deviation from the baseline. It is also worthwhile to mention that due to supercooling effects, the corresponding temperatures registered on heating and cooling curves may differ considerably.

There may be more than one thermal event for a multiphase alloy (Fig. 3.1-b). In such cases, we used the extrapolated onset ($T_{\text{extrapolated}}$) for the thermal events before melting, the invariant reactions, and the peak temperature (T_{peak}) for the liquidus temperature. The reason is that the flatness of the baseline is often not recovered after the invariant reactions especially when the two events occur at close temperatures. The determined T_{onset} or equivalently $T_{\text{extrapolated}}$ in this case may considerably deviate from the phase transition temperature. On cooling, however, the $T_{\text{extrapolated}}$ was used for all events because the deviations from the baseline were sharp for all thermal events.

Scheil solidification simulation: To interpret the solidification behaviour of the ternary alloys from the DTA results we used the Scheil solidification simulations [39] along with full-equilibrium calculations. In the Scheil approach it is assumed that the solid phases are frozen and the diffusion only occurs in the liquid phase. This rather extreme approximation is helpful because during the DTA measurements one cannot be sure that the equilibrium is reached.

3.3 X-ray diffraction

X-Ray Diffraction (XRD) is used to determine the crystal structure of previously unknown phases. In this regard, both single-crystal and powder XRD provide complementary information to characterize the new phases. For multiphase samples, powder XRD is also used to detect coexisting phases and the relative phase amounts.

For powder XRD measurements, pieces of alloy samples are ground to a fine powder. Then, the powder is transferred to a quartz tube. The

evacuated tube is then closed and annealed at a temperature below the liquidus for a few days to relieve the strain produced in the sample due to grinding and hence to prevent the peaks from broadening. For single-crystal measurements, small pieces (with the size of a few hundreds of μm) of the fragmented sample are annealed in a similar fashion as the powder samples but often for a longer time period.

The diffraction pattern consists of peaks with different intensities. The coexistence of the phases is determined using the intensity patterns [36]. There are reference patterns of single phase samples in databases such as Pearson's crystal data [40]. The XRD pattern is compared to the reference patterns using automated software like JANA2006 [41] to detect the present phases in an alloy sample. The same peaks of a single-crystalline phase as those in the reference pattern appear in the diffraction pattern but there may be shifts in the peak positions depending on the alloy composition. In the case of multiphase samples, there will be peaks of all coexisting crystalline phases in the XRD pattern (some peaks may overlap). The relative intensity of the peaks of the involved phases is an indication of the phase amounts.

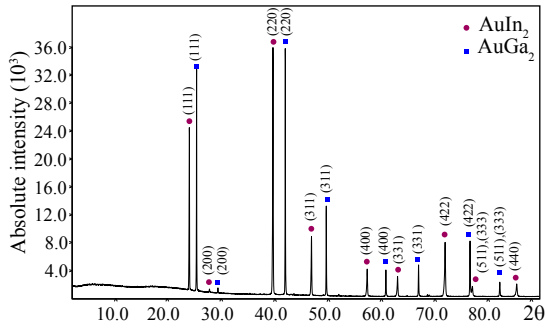

Figure 3.2: XRD pattern of a sample with the composition of 33.1% Au, 32.9% In, 34.0% Ga.

An XRD pattern for a two-phase sample consisting of $AuIn_2$ and $AuGa_2$ phases is shown in Fig. 3.2. Both phases have cubic structure meaning

that the diffraction pattern of both species is constituted of similar peaks. However, the reflections do not occur at similar angles due to difference in lattice parameters.

As it was pointed out, the crystal structure of the unknown phases can be characterized by the XRD data. For instance, the presence of a ternary phase cannot be detected only by extrapolation from binaries. However, when the ternary system is measured, XRD patterns of samples close in composition to that of the ternary phase will display extra peaks. The crystal structure and the lattice parameters of the new ternary phase are refined using the XRD powder data, while single-crystal data will reveal information on the site occupancies of atomic positions. Both these techniques were used to characterize the new ternary phase in the Au-In-Ga system [42].

3.4 Structural analysis

Indispensable phase diagram data can be obtained from microscopical and compositional analysis of the system. To pursue the former, either Scanning Electron Microscopy (SEM) or optical microscopy is used. For the latter, the Energy Dispersive X-ray Spectroscopy (EDS) technique can be implemented.

SEM micrographs reveal information on the number of phases for each sample. Moreover, the microstructures show the type of the invariant reaction for each alloy composition. In SEM, a collimated beam of high-energy electrons (5-20 KeV) bombard a previously polished and cleaned sample surface. In response, a number of species including secondary electrons, backscattered electrons and X-rays are ejected. Both the secondary and the backscattered electrons can create an image. Backscattered electrons are sensitive to the atomic number of the sample constituents, whereas secondary electrons create contrast due to surface topology [36]. A SEM micrograph of an alloy with the composition of 62.2% Au, 24.6% In, 13.2% Ga is shown in Fig. 3.3-a. There are three coexisting phases at this composition: AuGa, Au_3In_2 and Au_7In_3 forming through a eutectic reaction.

(a)

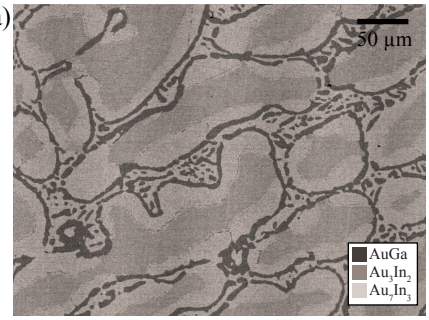

(b)

Phase	Au (at.%)	In (at.%)	Ga (at.%)
AuGa	54.0	2.0	44.0
Au_3In_2	63.6	31.6	4.8
Au_7In_3	69.8	26.0	4.2

Figure 3.3: (a) SEM micrograph and (b) EDS spectrum of an alloy with the composition of 62.2% Au, 24.6% In, 13.2% Ga.

SEM is often accompanied by X-ray spectroscopy making the compositional analysis possible simultaneously as the microstructural analysis. The resolution of the technique is limited to areas of the order of 1 μm^2 and hence finer microstructures than this limit cannot be detected [36]. The use of EDS for compositional analysis can be explained in connection with the microscopical analysis shown in Fig. 3.3-a. A small region of different phases (differentiated with shades of gray) were analysed using EDS to find the phase compositions. The compositional analysis (Fig. 3.3-b) indeed confirmed the presence of the same phases at this composition.

Using EDS, the solubility level of the phases can also be determined. For instance, the solubility of In in AuGa is 2 at.% at this composition. The spectrum of the AuGa phase in Fig. 3.3-b also shows that a fraction of Au species occupy In atomic positions.

Chapter 4

Au-In-Ga Ternary System

In this chapter, we will briefly discuss the assessment procedure of the Au-In-Ga ternary system. For more details, the reader is referred to Ref. [37, 42, 43].

The same methodology as summarized in Fig. 2.2 was followed to create a thermodynamic database for the Au-In-Ga ternary system. At first, an extensive literature search was conducted to find the available assessments or measurements on the ternary system and the sub-binaries.

The assessment of Au-In-Ga ternary system was lacking in the literature and the only available measurement on the system was restricted to the Au-rich part of the system [44]. The constituent binaries Au-Ga, Au-In and In-Ga, however, have previously been assessed [17–19, 45–51]. For the Au-Ga and In-Ga binaries, the parameters assessed by Wang et al. [17], and Anderson and Ansara [19] respectively were used. In the case of the Au-In system, all parameters were taken from the assessment by Liu et al. [18] except for one parameter which was modified from [18] due to the change in the unary description of the fcc-In phase in [46].

An isothermal section of the Au-In-Ga ternary at 280°C was constructed by extrapolating from the sub-binaries. Based on the calculated isothermal section, a number of alloy compositions were then chosen to perform measurements on the system using DTA, XRD, SEM and EDS techniques. In summary, a new ternary phase was detected. The solubility levels of the third element in binary phases were also detected using XRD and EDS. The liquidus and phase transition temperatures were found using the DTA results. The details of the experimental measurements are discussed in paper II [37].

The measurements displayed the presence of a new ternary phase, Au_2InGa_2,

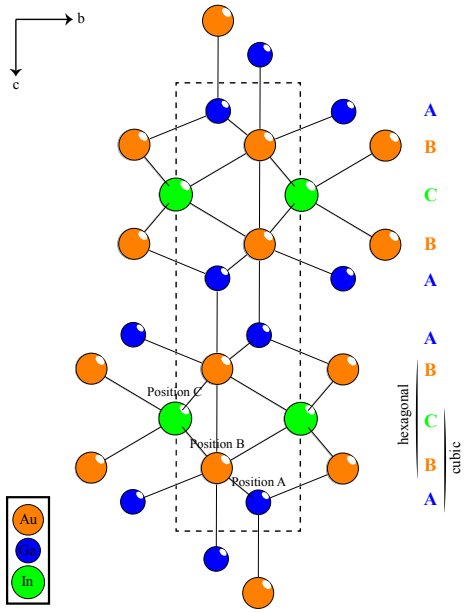

Figure 4.1: The unit cell of the new ternary phase Au_2InGa_2. The constituting atoms Au, In and Ga are illustrated with different colors, orange, green and blue, respectively. The dashed rectangle indicates the boundary of one unit cell. The geometric sequence is composed of ten layers: ABCBAABCBA while the atomic sequence comprises of five layers: GaAuInAuGa.

at about 40 at.% Au composition. The new ternary has an ordered close-packed structure with alternating hexagonal and cubic packing. The unit cell is isostructural to Pt_2Sn_3 [52] and is composed of four Au atoms, two In atoms and four Ga atoms. It has the lattice constants of $a = 4.20473(16)$Å and $c = 12.09673(5)$Å and belongs to the space group 194, $P6_3/mmc$. The two dimensional schematic of the unit cell of this phase in a direction is shown in Fig. 4.1. Only considering the geometry of the unit cell, strong homoatomic bonding due to presence of puckered Ga 6^3 nets and Au-Au dumbbells was primarily expected. However, subsequent first-principles cal-

culations of the electronic structure, to our surprise, showed that Au_2InGa_2 is stabilized due to strong interactions between the heteroatomic bonds Au-Ga and Au-In. The details of the crystal structure refinement and the electronic structure analysis are discussed in paper I [42].

In the next step, a three-sublattice model for the new ternary phase was adapted: $(Au)_{0.4}In_{0.2}(Ga)_{0.4}$. Since the ternary phase was an ordered phase, no solubility of the second element on the sublattices were considered. The models of the binary phases with substantial ternary solubility: AuIn, AuGa, $AuIn_2$ and $AuGa_2$ were also changed to include the observed solubility levels. The only ternary interaction parameter which was added to the description was the regular ternary interaction parameter of the liquidus phase. All phases in the Au-In-Ga ternary system and the corresponding Gibbs energy models are summarized in Table 4.1.

Finally, the optimization was performed in the PARROT module [34] of the Thermo-Calc software [35]. The PARROT optimizer works based on the least-squares fitting method in which the sum of squares of the errors [1] is minimized [5]. The optimization resulted in a set of self-consistent parameters which can reproduce most of the experimental data. The optimized database is displayed in the Appendix.

The details of the assessment is explained in paper III [43] where, using the optimized parameters, the diagram of liquidus projections is calculated and compared with the measured phase transition temperatures. Also, an isothermal section of the phase diagram at 280 °C and the diagram of monovariant lines are calculated.

[1] The error is the product of the difference between the calculated and observed quantities and a given weight to the observed quantity.

Table 4.1: All phases in the Au-In-Ga ternary system and the selected substitutional and sublattice models in the assessment according to the discussion in Section 2.2. In the current optimization, the ternary solubility in AuIn, $AuIn_2$, AuGa and $AuGa_2$ binary phases [37] were taken into account. The ternary interaction parameter for the liquid phase was also optimized. Moreover, the new ternary phase Au_2InGa_2 [42] was added to the system.

Phase	**Space group**	**Model**	**Phase**	**Space group**	**Model**
Liquid	-	(Au,Ga,In)	Au_7In_3	P-3	$(Au)_{.7}(In)_{.3}$
(Au)	Fm-3m	(Au,Ga,In)	Au_3In_2	P-3m1	$(Au)_{.5}(Au,In)_{.333}(In)_{.1667}$
(In)	I4/mmm	(In,Ga)	AuIn	P-1	$(Au)_{.5}(In,Ga)_{.5}$
(Ga)	cmc2	(Ga)	$AuIn_2$	Fm-3m	$(Au)_{.67}(In,Ga)_{.33}$
hcp	P63/mmc	(Au,Ga,In)	Au_7Ga_2-HT	P-62m	$(Au)_{.789}(In)_{.21}$
$d0_{24}$	P63/mmc	(Au,Ga,In)	Au_7Ga_2-LT	-	$(Au)_{.78}(In)_{.22}$
Au_4In-HT	-	$(Au)_{.785}(In)_{.215}$	Au_7Ga_3	-	$(Au)_{.7}(Ga)_{.3}$
Au_4In-Lt	P-3	$(Au)_{.78}(In)_{.22}$	AuGa	Pnma	$(Au)_{.5}(Ga,In)_{.5}$
Au_3In	Pmmn	$(Au)_{.75}(In)_{.25}$	$AuGa_2$	Fm-3m	$(Au)_{.67}(Ga,In)_{.33}$
Au_9In_4	P-43m	$(Au)_{.692}(Au,In)_{.231}(In)_{.076}$	Au_2InGa_2	P63/mmc	$(Au)_{.4}(In)_{.2}(Ga)_{.4}$

Chapter 5

Summary and Outlook

In this work, a thermodynamic database for the Au-In-Ga system was developed using the CALPHAD technique. Due to the lack of measured data on this ternary system in the literature, it was measured using the relevant techniques for collecting the phase diagram data including DTA, XRD, SEM and EDS. As a result, a previously unknown ternary phase with a new type structure was identified. The phase transition temperatures and the ternary solubilities were also detected. All the experimental measurements were used to adjust the model parameters of the Gibbs energy of phases, leading to an optimized set of parameters.

The thermodynamic description of this particular ternary system will be useful to understand the state of the seed particle in the growth of heterostructure III-V nanowires containing Ga and and In and seeded by gold particles. However, in the future, the database can be extended to include the group V elements as well. This is not a big issue because the powerful CALPHAD technique enables us to extrapolate to higher order systems with a minimal need for measurements. The database can be further optimized to include the size and even shape of the system. This will make the thermodynamic database particularly suitable to describe the growth of relevant nanoscale structures.

Bibliography

[1] R. Yan, D. Gargas, and P. Yang. Nanowire photonics. *Nat. Photonics*, 3(10):569–576, 2009.

[2] L. E. Wernersson, C. Thelander, E. Lind, and L. Samuelson. III-V nanowires–extending a narrowing road. *P IEEE*, 98(12):2047–2060, 2010.

[3] R. S. Wagner and W. C. Ellis. Vapor-Liquid-Solid mechanism of single crystal growth. *Appl. Phys. Lett.*, 4(89):89–90, 1964.

[4] E. J. Schwalbach and P. W. Voorhees. Doping nanowires grown by the vapor-liquid-solid mechanism. *Appl. Phys. Lett.*, 95(6):063105, 2009.

[5] H. L. Lukas, S.G. Fries, and B. Sundman. *Computational Thermodynamics: The Calphad Method*. Cambridge Uni. press, 2007.

[6] M. Paladugu, J. Zou, Y. Guo, X. Zhang, Y. Kim, H. J. Joyce, Q. Gao, H. H. Tan, and C. Jagadish. Nature of heterointerfaces in GaAs/InAs and InAs/GaAs axial nanowire heterostructures. *Appl. Phys. Lett.*, 93(10):101911, 2008.

[7] K. A. Dick, J. Bolinsson, B. M. Borg, and J. Johansson. Controlling the abruptness of axial heterojunctions in III-V nanowires: Beyond the reservoir effect. *Nano Lett.*, 12(6):3200–3206, 2012.

[8] Y. Guo, H. Xu, G. J. Auchterlonie, T. Burgess, H. J. Joyce, Q. Gao, H. H. Tan, C. Jagadish, H. Shu, X. Chen, W. Lu, Y. Kim, and J. Zou. Phase separation induced by Au catalysts in ternary InGaAs nanowires. *Nano Lett.*, 13(2):643–650, 2013.

[9] R. Vallee, M. Wautelet, J. P. Dauchot, and M. Hecq. Size and segregation effects on the phase diagrams of nanoparticles of binary systems. *Nanotechnology*, 12(1):68, 2001.

[10] G. Abudukelimu, G. Guisbiers, and M. Wautelet. Theoretical phase diagrams of nanowires. *J. Mater. Res.*, 21:2829–2834, 11 2006.

[11] E. J. Schwalbach and P. W. Voorhees. Phase equilibrium and nucleation in VLS-grown nanowires. *Nano Letters*, 8(11):3739–3745, 2008.

[12] J. Pohl, C. Stahl, and K. Albe. Size-dependent phase diagrams of metallic alloys: A Monte Carlo simulation study on order-disorder transitions in Pt-Rh nanoparticles. *Beilstein J. Nanotechnol.*, 3:1–11, 2012.

[13] J. Lee and K. J. Sim. General equations of Calphad-type thermodynamic description for metallic nanoparticle systems. *Calphad*, 44:129 – 132, 2014.

[14] E. Sutter and P. Sutter. Phase diagram of nanoscale alloy particles used for Vapor-Liquid-Solid growth of semiconductor nanowires. *Nano Letters*, 8(2):411–414, 2008.

[15] B. J. Kim, J. Tersoff, C.-Y. Wen, M. C. Reuter, E. A. Stach, and F. M. Ross. Determination of size effects during the phase transition of a nanoscale Au-Si eutectic. *Phys. Rev. Lett.*, 103 (15):155701–4, 2009.

[16] E. A. Sutter and P. W. Sutter. Size-dependent phase diagram of nanoscale alloy drops used in Vapor-Liquid-Solid growth of semiconductor nanowires. *ACS Nano*, 4(8):4943–4947, 2010.

[17] J. Wang, Y. J. Liu, L. B. Liu, H. Y. Zhou, and Z. P. Jin. Thermodynamic assessment of the Au-Ga binary system. *Calphad*, 35(2):242–248, 2011.

[18] S. Liu, Y. Cui, K. Ishida, and Z. Jin. Thermodynamic reassessment of the Au–In binary system. *Calphad*, 27(1):27–37, 2003.

[19] T. J. Anderson and I. Ansara. The Ga–In (Gallium-Indium) system. *J. Phase Equilib.*, 12(1):64–72, 1991.

[20] L. Kaufman and H. Bernstein. *Computer Calculations of Phase Diagrams*. New York: Academic Press, 1970.

[21] J. J. van Laar. *Z. Phys. Chem.*, 63:216, 1908.

[22] J. J. van Laar. *Z. Phys. Chem.*, 64:257, 1908.

[23] C. Wagner. *Thermodynamics of alloys.* Addison-Wesley Press, 1952.

[24] R. Ferro and G. Cacciamani. Remarks on crystallochemical aspects in thermodynamic modeling. *Calphad*, 26(3):439 – 458, 2002.

[25] Z. K. Liu. First-principles calculations and Calphad modeling of thermodynamics. *J. Phase Equilib.*, 30(5):517–534, 2009.

[26] M. Hillert. The compound energy formalism. *J. Alloys Compd.*, 320(2):161 – 176, 2001.

[27] L. Kaufman. The lattice stability of metals. I. Titanium and Zirconium. *Acta Metall.*, 7(8):575 – 587, 1959.

[28] SGTE unary database ver. 4.4. *Updated from: A. T. Dinsdale, Calphad 15, 1991,317.*

[29] O. Redlich and A. T. Kister. Algebraic representation of thermodynamic properties and the classification of solutions. *Indust. Eng. Chem.*, 40(2):345–348, 1948.

[30] Y. M. Muggianu, M. Gambino, and J. P. Bos. Enthalpies of formation of liquid bismuth-gallium-tin alloys at 723 K. Choice of an analytical representation of integral and partial thermodynamic functions of mixing. *J. Chim. Phys. Physicochim. Biol.*, 72:83–89, 1975.

[31] P. Chartrand and A. D. Pelton. On the choice of geometric thermodynamic models. *J. Phase Equilib.*, 21(2):141–147, 2000.

[32] A. D. Pelton. A general geometric thermodynamic model for multicomponent solutions. *Calphad*, 25(2):319 – 328, 2001.

[33] R. Schmid-Fetzer, D. Andersson, P. Y. Chevalier, L. Eleno, O. Fabrichnaya, U. R. Kattner, B. Sundman, C. Wang, A. Watson, L. Zabdyr,

and M Zinkevich. Assessment techniques, database design and software facilities for thermodynamics and diffusion. *Calphad*, 31(1):38–52, 2007.

[34] B. Sundman, B. Jansson, and J. O. Andersson. The Thermo-Calc databank system. *Calphad*, 9(2):153 – 190, 1985.

[35] J. O. Andersson, T. Helander, L. Höglund, P. Shi, and B. Sundman. Thermo-Calc & DICTRA, computational tools for materials science. *Calphad*, 26(2):273–312, 2002.

[36] J.-C. Zhao, editor. *Methods for Phase Diagram Determination*. Elsevier, 2007.

[37] M. Ghasemi, S. Lidin, and J. Johansson. The phase equilibria in the Au-In-Ga ternary system. *J. Alloys Compd.*, 588:474–480, 2014.

[38] W.J. Boettinger and U.R. Kattner. On differential thermal analyzer curves for the melting and freezing of alloys. *Metall. Mater. Trans. A*, 33(6):1779–1794, 2002.

[39] M.C. Flemings. Solidification processing. *Metall. Trans.*, 5(10):2121–2134, 1974.

[40] P. Villars and K. Cenzual. Pearson's crystal data: Crystal structure database for inorganic compounds (on DVD). Release 2012-13, ASM International ®, Materials Park, Ohio, USA.

[41] V. Petricek, M. Dusek, and L. Palatinus. Jana2006. The crystallographic computing system. Institute of Physics, Praha, Czech Republic.

[42] M. Ghasemi, S. Lidin, J. Johansson, and F. Wang. Bonding in intermetallics may be deceptive- The case of the new type structure Au_2InGa_2. *Intermetallics*, 46:40–44, 2014.

[43] M. Ghasemi, B. Sundman, S. G. Fries, and J. Johansson. The thermodynamic assessment of the Au-In-Ga system. *J. Alloys Compd.*, 600:178 – 185, 2014.

[44] R. F. Hoyt and A. C. Mota. Elastic strain energy dependence of Tc in ternary goldbased solid solutions. *J. Less Common Met.*, 62:183–188, 1978.

[45] J. Liu, C. Guo, C. Li, and Z. Du. Thermodynamic assessment of the Au-Ga system. *J. Alloys Compd.*, 508(1):62–70, 2010.

[46] D. Boa and I Ansara. Thermodynamic assessment of the ternary system Bi-In-Pb. *Thermochimica Acta*, 314(1–2):79 – 86, 1998.

[47] F. H. Hayes and O. Kubaschewski. A reassessment of the system Indium–Gallium. *J. Inst. Met.*, 97:381–383, 1969.

[48] M. V. Rao and W. A. Tiller. The system In–Ga: Thermodynamics and computed phase equilibria. *J. Mat. Sci.*, 7(1):14–18, 1972.

[49] I. Ansara, J. P. Bros, and C. Girard. Thermodynamic analysis of the Ga–In, Al–Ga, Al–In and the Al–Ga–In systems. *Calphad*, 2(3):187–196, 1978.

[50] B. C. Rugg and T. G. Chart. A critical assessment of thermodynamic and phase diagram data for the Gallium-Indium system. *Calphad*, 14(2):115–123, 1990.

[51] S. R. Ravindra and J. P. Hajra. Thermodynamics and phase equilibria in the system Ga-In using multi-parameter functions. *Calphad*, 17(2):151–156, 1993.

[52] K. Schubert and H. Pfisterer. Kristallstruktur von Pt_2Sn_3. *Z. Metallkd*, 40:405–411, 1949.

Appendix: Au-In-Ga database

```
$ Database for ternary Au-In-Ga system
$ ------------------------------------------------------------------------
$ TDB file created by Masoomeh Ghasemi
$
$ Solid State Physics, Lund University, Sweden
$
$ E-mail: masoomeh.ghasemi@ftf.lth.se
$ ------------------------------------------------------------------------
$
$ Au-In parameter set, except for G(FCC_A1,AU,IN;1) is taken from:
$ Thermodynamic Reassessment of the Au-In Binary System.
$ H.S.Liu, Y.Cui, K.Ishida, Z.P.Jin, CALPHAD, 27 (2003) 27-37.
$
$ Au-Ga parameter set is taken from:
$ Thermodnamic assessment of the Au-Ga binary sysem.
$ J. Wang, Y. J. Liu, L. B. Liu, H.Y. Zhou, Z. P. Jin,
$ CALPHAD, 35 (2011) 242-248.
$
$ In-Ga parameter set is taken from:
$ The Ga-In (gallium-indium) system.
$ J. Anderson and I. Ansara, J. Phase Equilib., 12 (1991) 64-72.
$
$ G(FCC_A1,AU,IN;1), the ternary liquidus parameter and parameters
$ for the ternary phase are taken from:
$ The thermodynamic assessment of the Au-In-Ga system.
$ M. Ghasemi, B. sundman, S. G. Fries, J. Johansson,
$ J. Alloys Compd., 600 (2014) 178-185.
$
$ ------------------------------------------------------------------------
 ELEMENT /-   ELECTRON_GAS              0.0000E+00  0.0000E+00  0.0000E+00!
 ELEMENT VA   VACUUM                    0.0000E+00  0.0000E+00  0.0000E+00!
 ELEMENT AU   FCC_A1                    1.9697E+02  0.0000E+00  0.0000E+00!
 ELEMENT GA   ORTHORHOMBIC_CMCA         6.9723E+01  0.0000E+00  0.0000E+00!
 ELEMENT IN   TETRAGONAL_A6             1.1482E+02  0.0000E+00  0.0000E+00!



 FUNCTION GHSERAU   298.15 -6938.853+106.830495*T-22.75455*T*LN(T)
     -.00385924*T**2+3.79625E-07*T**3-25097*T**(-1); 933.51 Y
      -93575.261+1021.60143*T-155.6947*T*LN(T)+.08756015*T**2
     -1.1518713E-05*T**3+1063721O*T**(-1); 1337.58 Y
      +314062.987-2016.37379*T+263.2523*T*LN(T)-.11821685*T**2
     +8.923845E-06*T**3-67999850*T**(-1); 1735.80 Y
      -12138.657+165.277268*T-30.9616*T*LN(T); 3200 N !
 FUNCTION GHSERIN   298.15 -6978.89+92.338115*T-21.8386*T*LN(T)
```

```
     -.00572566*T**2-2.120321E-06*T**3-22906*T**(-1); 429.78 Y
      -7033.47+124.476492*T-27.4562*T*LN(T)+5.4607E-04*T**2-8.367E-08*T**3
     -211708*T**(-1)+3.30026E+22*T**(-9); 3200 N !
 FUNCTION GHSERGA   298.15 -21312.331+585.263691*T-108.228783*T*LN(T)
     +.227155636*T**2-1.18575257E-04*T**3+439954*T**(-1); 302.91 Y
      -7055.643+132.73019*T-26.0692906*T*LN(T)+1.506E-04*T**2
     -4.0173E-08*T**3-118332*T**(-1)+1.64547E+23*T**(-9); 4000 N !
 FUNCTION UN_ASS    298.15 +0.0; 300 N !

 TYPE_DEFINITION % SEQ *!
 DEFINE_SYSTEM_DEFAULT ELEMENT 2 !
 DEFAULT_COMMAND DEF_SYS_ELEMENT VA /- !

$------------------------------------------------------------------------------
$ PARAMETERS FOR LIQUID PHASE
$------------------------------------------------------------------------------
 PHASE LIQUID:L %  1  1.0  !
    CONSTITUENT LIQUID:L :AU,GA,IN :  !

   PARAMETER G(LIQUID,AU;0)              298.15 +12552-9.38411*T+GHSERAU#;
  3200 N REF0 !
   PARAMETER G(LIQUID,GA;0)              200 -15821.033+567.189696*T
  -108.228783*T*LN(T)+.227155636*T**2-1.18575257E-04*T**3+439954*T**(-1)
  -7.0171E-17*T**7; 302.91 Y
   -1389.188+114.049043*T-26.0692906*T*LN(T)+1.506E-04*T**2-4.0173E-08*T**3
  -118332*T**(-1); 4000 N REF0 !
   PARAMETER G(LIQUID,IN;0)              298.15 -3696.798+84.701255*T
  -21.8386*T*LN(T)-.00572566*T**2-2.120321E-06*T**3-22906*T**(-1)
  -5.59058E-20*T**7; 429.75 Y
   -3749.81+116.835784*T-27.4562*T*LN(T)+5.4607E-04*T**2-8.367E-08*T**3
  -211708*T**(-1); 3800 N REF0 !
   PARAMETER G(LIQUID,AU,GA;0)           298.15 -71830.123+42.286*T
  -4.289*T*LN(T); 6000 N REF0 !
   PARAMETER G(LIQUID,AU,GA;1)           298.15 -22892.323+5.069*T; 6000 N
  REF0 !
   PARAMETER G(LIQUID,AU,GA;2)           298.15 -8839.911+7.674*T; 6000 N
  REF0 !
   PARAMETER G(LIQUID,AU,GA,IN;0)        298.15 +20500; 6000 N REF0 !
   PARAMETER G(LIQUID,AU,IN;0)           298.15 -76196.19+64.2914*T
  -6.6375*T*LN(T); 6000 N REF0 !
   PARAMETER G(LIQUID,AU,IN;1)           298.15 -31134.02+81.3582*T
  -8.5134*T*LN(T); 6000 N REF0 !
   PARAMETER G(LIQUID,GA,IN;0)           298.15 +4450+1.19185*T; 3000 N !
   PARAMETER G(LIQUID,GA,IN;1)           298.15 +.259*T; 3000 N !

$------------------------------------------------------------------------------
$ PARAMETERS FOR Au2InGa2 TERNARY PHASE
$------------------------------------------------------------------------------
```

```
 PHASE AU2GA2IN  %  3 .4   .4   .2 !
    CONSTITUENT AU2GA2IN  :AU : GA : IN :  !

   PARAMETER G(AU2GA2IN,AU:GA:IN;0)       298.15 -35900+22.5*T+.4*GHSERAU#
  +.4*GHSERGA#+.2*GHSERIN#; 3000 N REF0 !

$----------------------------------------------------------------------------
$ PARAMETERS FOR AU3IN PHASE
$----------------------------------------------------------------------------
 PHASE AU3IN  %  2 .75   .25 !
    CONSTITUENT AU3IN  :AU : IN :  !

   PARAMETER G(AU3IN,AU:IN;0)             298.15 -10582.67-2.9323*T
  +.75*GHSERAU#+.25*GHSERIN#; 6000 N REF0 !

$----------------------------------------------------------------------------
$ PARAMETERS FOR AU7GA2_H PHASE
$----------------------------------------------------------------------------
 PHASE AU7GA2_H  %  2 .789476   .210526 !
    CONSTITUENT AU7GA2_H  :AU : GA :  !

   PARAMETER G(AU7GA2_H,AU:GA;0)          298.15 -11148.55-1.257*T
  +.789476*GHSERAU#+.210526*GHSERGA#; 6000 N REF0 !

$----------------------------------------------------------------------------
$ PARAMETERS FOR AU7GA2_L PHASE
$----------------------------------------------------------------------------
 PHASE AU7GA2_L  %  2 .777773   .222227 !
    CONSTITUENT AU7GA2_L  :AU : GA :  !

   PARAMETER G(AU7GA2_L,AU:GA;0)          298.15 -12640.544+.326*T
  +.777773*GHSERAU#+.222227*GHSERGA#; 6000 N REF0 !

$----------------------------------------------------------------------------
$ PARAMETERS FOR AU7GA3 PHASE
$----------------------------------------------------------------------------
 PHASE AU7GA3  %  2 .7   .3 !
    CONSTITUENT AU7GA3  :AU : GA :  !

   PARAMETER G(AU7GA3,AU:GA;0)            298.15 -16720.107+2.397*T
  +.7*GHSERAU#+.3*GHSERGA#; 6000 N REF0 !


$----------------------------------------------------------------------------
$ PARAMETERS FOR AU7IN3 PHASE
$----------------------------------------------------------------------------
 PHASE AU7IN3  %  2 .7   .3 !
```

```
    CONSTITUENT AU7IN3  :AU : IN :  !

   PARAMETER G(AU7IN3,AU:IN;0)            298.15 -12813.11-2.0538*T
  +.7*GHSERAU#+.3*GHSERIN#; 6000 N REF0 !

$----------------------------------------------------------------------------
$ PARAMETERS FOR AUGA PHASE
$----------------------------------------------------------------------------
 PHASE AUGA1  %  2 .5   .5 !
    CONSTITUENT AUGA1  :AU% : GA%,IN :  !

   PARAMETER G(AUGA1,AU:GA;0)             298.15 -24002.418+4.422*T
  +.5*GHSERAU#+.5*GHSERGA#; 6000 N REF0 !
   PARAMETER G(AUGA1,AU:IN;0)             298.15 +20000+.5*GHSERAU#
  +.5*GHSERIN#; 6000 N REF0 !
   PARAMETER G(AUGA1,AU:GA,IN;0)          298.15 -37500; 6000 N REF0 !

$----------------------------------------------------------------------------
$ PARAMETERS FOR AUIN PHASE
$----------------------------------------------------------------------------
 PHASE AUIN1  %  2 .5   .5 !
    CONSTITUENT AUIN1  :AU% : GA,IN% :  !

   PARAMETER G(AUIN1,AU:GA;0)             298.15 +20000+.5*GHSERAU#
  +.5*GHSERGA#; 6000 N REF0 !
   PARAMETER G(AUIN1,AU:IN;0)             298.15 -20188.37+2.3786*T
  +.5*GHSERAU#+.5*GHSERIN#; 6000 N REF0 !
   PARAMETER G(AUIN1,AU:GA,IN;0)          298.15 -39500; 6000 N REF0 !

$----------------------------------------------------------------------------
$ PARAMETERS FOR AUX2 PHASE
$----------------------------------------------------------------------------
 PHASE AUX2  %  2 .33333   .66667 !
    CONSTITUENT AUX2  :AU% : GA%,IN :  !

   PARAMETER G(AUX2,AU:GA;0)              298.15 -24823.663+5.961*T
  +.333333*GHSERAU#+.666667*GHSERGA#; 6000 N REF0 !
   PARAMETER G(AUX2,AU:IN;0)              298.15 -26129.06+11.1133*T
  +.333333*GHSERAU#+.666667*GHSERIN#; 6000 N REF0 !
   PARAMETER G(AUX2,AU:GA,IN;0)           298.15 8900; 6000 N REF0 !

$----------------------------------------------------------------------------
$ PARAMETERS FOR AU4IN_H PHASE
$----------------------------------------------------------------------------
 PHASE BETA_0  %  2 .785   .215 !
    CONSTITUENT BETA_0  :AU : IN :  !

   PARAMETER G(BETA_0,AU:IN;0)            298.15 -8980.42-3.3042*T
```

```
  +.785*GHSERAU#+.215*GHSERIN#; 6000 N REF0 !

$----------------------------------------------------------------------------
$ PARAMETERS FOR AU4IN_L PHASE
$----------------------------------------------------------------------------
 PHASE BETA_1  %  2 .77778   .22222 !
    CONSTITUENT BETA_1  :AU : IN :  !

   PARAMETER G(BETA_1,AU:IN;0)            298.15 -9382.52-3.1015*T
  +.77778*GHSERAU#+.22222*GHSERIN#; 6000 N REF0 !

$----------------------------------------------------------------------------
$ PARAMETERS FOR AU9IN4 PHASE
$----------------------------------------------------------------------------
 PHASE GAMMA  %  3 .69231   .23077   .07692 !
    CONSTITUENT GAMMA  :AU : AU,IN : IN :  !

   PARAMETER G(GAMMA,AU:AU:IN;0)          298.15 -2830.47-2.5191*T
  +.92398*GHSERAU#+.07692*GHSERIN#; 6000 N REF0 !
   PARAMETER G(GAMMA,AU:IN:IN;0)          298.15 -11992.16-3.6511*T
  +.69231*GHSERAU#+.30769*GHSERIN#; 6000 N REF0 !
   PARAMETER G(GAMMA,AU:AU,IN:IN;0)       298.15 +2144.6; 6000 N REF0 !

$----------------------------------------------------------------------------
$ PARAMETERS FOR AU3IN2 PHASE
$----------------------------------------------------------------------------
 PHASE PSI  %  3 .5   .33333   .16667 !
    CONSTITUENT PSI  :AU : AU,IN : IN :  !

   PARAMETER G(PSI,AU:AU:IN;0)            298.15 +2153.38-8.039*T
  +.83333*GHSERAU#+.16667*GHSERIN#; 6000 N REF0 !
   PARAMETER G(PSI,AU:IN:IN;0)            298.15 -18225.14+3*T+.5*GHSERAU#
  +.5*GHSERIN#; 6000 N REF0 !
   PARAMETER G(PSI,AU:AU,IN:IN;0)         298.15 -15683.16; 6000 N REF0 !

$----------------------------------------------------------------------------
$ PARAMETERS FOR FCC_A1 PHASE
$----------------------------------------------------------------------------
 PHASE FCC_A1  %  1  1.0  !
    CONSTITUENT FCC_A1  :AU,GA,IN :  !

   PARAMETER G(FCC_A1,AU;0)               298.15 +GHSERAU#; 3200 N REF0 !
   PARAMETER G(FCC_A1,GA;0)               200 -17512.331+575.063691*T
  -108.228783*T*LN(T)+.227155636*T**2-1.18575257E-04*T**3+439954*T**(-1);
  302.91 Y
   -3255.643+122.53019*T-26.0692906*T*LN(T)+1.506E-04*T**2-4.0173E-08*T**3
  -118332*T**(-1)+1.64547E+23*T**(-9); 4000 N REF0 !
   PARAMETER G(FCC_A1,IN;0)               298.15 GHSERIN#+162.061;
```

```
3800 N REF0 !
   PARAMETER G(FCC_A1,AU,IN;0)            298.15 -48493.65+46.6237*T
  -6.8308*T*LN(T); 6000 N REF0 !
   PARAMETER G(FCC_A1,AU,IN;1)            298.15 +200; 6000 N REF0 !
   PARAMETER G(FCC_A1,AU,GA;0)            200 -31511.768-12.788*T; 4000 N
  REF0 !
   PARAMETER G(FCC_A1,AU,GA;1)            200 -20073.352+14.067*T; 4000 N
  REF0 !
   PARAMETER G(FCC_A1,GA,IN;0)            200 +25000; 4000 N REF0 !


$---------------------------------------------------------------------------
$ PARAMETERS FOR HCP PHASE
$---------------------------------------------------------------------------
 PHASE HCP  %  1  1.0  !
    CONSTITUENT HCP  :AU,GA,IN :  !

   PARAMETER G(HCP,AU;0)                  298.15 -6698.106+108.430098*T
  -22.75455*T*LN(T)-.00385924*T**2+3.79625E-07*T**3-25097*T**(-1); 929.40 Y
   -93345.731+1023.29543*T-155.706745*T*LN(T)+.08756015*T**2
  -1.1518713E-05*T**3+10637210*T**(-1); 1337.33 Y
   +314308.579-2014.77825*T+263.252259*T*LN(T)-.118216828*T**2
  +8.923844E-06*T**3-67999832*T**(-1); 1735.80 Y
   -11893.033+166.872524*T-30.9616*T*LN(T); 3200 N REF0 !
   PARAMETER G(HCP,GA;0)                  200 -16812.331+575.763691*T
  -108.228783*T*LN(T)+.227155636*T**2-1.18575257E-04*T**3+439954*T**(-1);
  302.91 Y
   -2555.643+123.23019*T-26.0692906*T*LN(T)+1.506E-04*T**2-4.0173E-08*T**3
  -118332*T**(-1)+1.64547E+23*T**(-9); 4000 N REF0 !
   PARAMETER G(HCP,IN;0)                  298.15 -6445.89+91.651315*T
  -21.8386*T*LN(T)-.00572566*T**2-2.120321E-06*T**3-22906*T**(-1); 429.75 Y
   -6500.516+123.789788*T-27.4562*T*LN(T)+5.4607E-04*T**2-8.367E-08*T**3
  -211708*T**(-1)+3.53116E+22*T**(-9); 3800 N REF0 !
   PARAMETER G(HCP,AU,IN;0)               298.15 -55780.55+13.8198*T; 6000 N
  REF0 !
   PARAMETER G(HCP,AU,IN;1)               298.15 +6788.95-32.893*T; 6000 N
  REF0 !
   PARAMETER G(HCP,AU,GA;0)               298.15 +25000; 6000 N REF0 !
   PARAMETER G(HCP,GA,IN;0)               298.15 +25000; 6000 N REF0 !

$---------------------------------------------------------------------------
$ PARAMETERS FOR D024 PHASE
$---------------------------------------------------------------------------
 PHASE D024  %  1  1.0  !
    CONSTITUENT D024  :AU,GA,IN :  !

   PARAMETER G(D024,AU;0)                 298.15 +125+.79*T+GHSERAU#; 6000 N
  REF0 !
```

```
   PARAMETER G(D024,GA;0)                 298.15 +4500-9.5*T+GHSERGA#; 6000
  N REF0 !
   PARAMETER G(D024,IN;0)                 298.15 +520-.384*T+GHSERIN#; 3800
  N REF0 !
   PARAMETER G(D024,AU,GA;0)              298.15 -41291.692-.227*T; 6000 N
  REF0 !
   PARAMETER G(D024,AU,GA;1)              298.15 -15367.206-3.768*T; 6000 N
  REF0 !
   PARAMETER G(D024,AU,IN;0)              298.15 -48238.66+5.3551*T; 6000 N
  REF0 !
   PARAMETER G(D024,AU,IN;1)              298.15 -48.36-16.7932*T; 6000 N
  REF0 !
   PARAMETER G(D024,GA,IN;0)              298.15 +25000; 6000 N REF0 !

$----------------------------------------------------------------------------
$ PARAMETERS FOR GA-ORTHORHOMBIC PHASE
$----------------------------------------------------------------------------
 PHASE ORTHORHOMBIC  %  1  1.0  !
    CONSTITUENT ORTHORHOMBIC  :GA :  !

   PARAMETER G(ORTHORHOMBIC,GA;0)         298.15 +GHSERGA#; 4000 N REF0 !

$----------------------------------------------------------------------------
$ PARAMETERS FOR IN_TETRAGONAL PHASE
$----------------------------------------------------------------------------
 PHASE TETRAGONAL_A6  %  1  1.0  !
    CONSTITUENT TETRAGONAL_A6  :GA,IN :  !

   PARAMETER G(TETRAGONAL_A6,GA;0)        200 -17466.331+575.463691*T
  -108.228783*T*LN(T)+.227155636*T**2-1.18575257E-04*T**3+439954*T**(-1);
  302.91 Y
   -3209.643+122.93019*T-26.0692906*T*LN(T)+1.506E-04*T**2-4.0173E-08*T**3
  -118332*T**(-1)+1.64547E+23*T**(-9); 4000 N REF0 !
   PARAMETER G(TETRAGONAL_A6,IN;0)        298.15 +GHSERIN#; 3200 N REF0 !
   PARAMETER G(TETRAGONAL_A6,GA,IN;0)     298.15 +9000; 6000 N REF0 !

 LIST_OF_REFERENCES
 NUMBER  SOURCE
  !
```

Lund University